Optimal Design and Wind Tunnel Testing of Propellers for a Winged Compound Helicopter

Keita Kimura, Japan Aerospace Exploration Agency (JAXA), Mitaka, Tokyo, Japan
Hideaki Sugawara, Japan Aerospace Exploration Agency (JAXA), Mitaka, Tokyo, Japan
Yasutada Tanabe, Japan Aerospace Exploration Agency (JAXA), Mitaka, Tokyo, Japan

Abstract

This paper presents an example of optimal propeller designs for a winged compound helicopter and its experimental/numerical validations. Considering flight conditions of the full-scale aircraft, a conceptual design of the propeller specifications has been conducted. The chord and twist distributions are optimized using Efficient Global Optimization (EGO) with a Kriging model, and the optimal propeller shapes are explored through performance evaluation using CFD analysis. While previous research focused on the design of side propellers, this study reports on the design of the tail propeller. Additionally, the performance of the optimal designs has been evaluated based on wind tunnel test results and CFD analysis. The fuel-saving effects of these optimal propellers on the rotorcraft system are also assessed, showing approximately a 10% reduction in fuel consumption at target cruise condition based on both CFD and wind tunnel test results.

1. NOTATIONS

c	: chord length
c_{eq}	: equivalent chord length
C_T	: thrust coefficient (= $T/\rho\pi R^2 V_{tip}^2$)
C_T/σ	: blade loading
C_Q	: torque coefficient (= $Q/\rho\pi R^3 V_{tip}^2$)
C_P	: power coefficient (= $P/\rho\pi R^2 V_{tip}^3$)
D	: wind-axis drag force
D_e	: effective drag force (= $D + P/V$)
F	: force (mainly side force)
FoM	: Figure of merit (= $C_T^{1.5}/\sqrt{2}C_P$)
L/D_e	: effective lift to drag ratio of rotor
J	: advance ratio for propeller (= $V/2nR$)
M_{tip}	: tip Mach number
n	: rotational speed [rps]
P	: power
Q	: torque
R	: radius of blade
T	: thrust
V	: speed of aircraft / speed of wind tunnel flow
V_{tip}	: blade tip speed
ρ	: air density
ω	: angular velocity
μ	: advance ratio for main rotor
σ	: blade solidity
η	: propeller efficiency (= TV/P)

Subscript

$\square_{MR}$	: main rotor
$\square_{SP}$	: side propeller
$\square_{TP}$	: tail propeller
$\square_{fin}$	: vertical/horisontal stabilizer
$\square_{adv}$	: advancing side
$\square_{ret}$	: retreating side
$\square_{hv}$	: hovering
$\square_{FF}$	: cruise (forward flight)

2. INTRODUCTION

2.1. Recent developments of high-speed helicopters

In JAXA, the pursuit of a high-speed helicopter aims to achieve approximately twice the conventional flight speed (500 km/h) with the same fuel consumption per unit distance [1]. The proposed compound helicopter has a single main rotor and fixed wings that produce lift, and the propulsion forces are generated via tail/side propellers and maintaining yaw attitude with side propellers. Among the technical challenges for this rotorcraft, one lies in the reasonable design of propellers that achieve high fuel efficiency without missing its flyability. Such advancements should contribute to the performance enhancement of upcoming compound helicopters such as Airbus' RACER [2], Sikorsky/Boeing's SB>1 Defiant [3], and domestically, Kawasaki Heavy Industries' unmanned VTOL aircraft, K-RACER [4] (Compound Type) and so on.

2.2. Optimal design studies for rotor blades

In recent years, significant improvements in computational capability have enabled the application of optimization techniques such as genetic algorithms and particle swarm optimization to rotorcraft design. The optimization method adopted by JAXA combines the Kriging response surface model with Efficient Global Optimization (EGO) [5]. Regarding optimization methods, mutual validation for a common optimization problem is being conducted in collaboration with DLR and NERA as reported in [6] [7] [8].

In addition to the optimization methods themselves, a fundamental issue lies in how design variables and evaluation functions are defined. In rotor designs, various metrics related to aerodynamics, structure, and acoustics are typically established as evaluation functions. For optimizing aerodynamic performance, evaluation functions like hover efficiency (Figure of Merit) and effective lift to drag ratio (L/D_e) are commonly used, with parameters such as chord length and twist angle being determined. As examples of blade design, the HSHER blade, modified by Sikorsky for improved forward flight performance in high speed [9], and Airbus's ERATO/Blue Edge [10], enhanced for reduced BVI noise through the addition of a double-swept angle, can be mentioned. In the last decade, JAXA has been advancing in the optimal design of main rotor blade for high advance ratio flight to establish numerical analysis-based optimal design techniques [11] [12]

2.3. Scope and objectives

In this paper, a conceptual design and planform optimization of a tail propeller for a winged compound helicopter are conducted in order to obtain an optimal solution that shows potential performance improvements over the baseline propeller. Furthermore, the optimized propellers are manufactured at a 1/7 scale of the full-scale, and their performance are validated through wind tunnel testing (and also CFD analysis), demonstrating that the optimally designed propellers meet the expected performance criteria.

Through these activities, the validity of the design methodology has been confirmed, and the power reduction effects when equipping with the optimally designed propellers are investigated. The impact on the overall system power is also evaluated.

3. METHODOLOGY

3.1. Optimization workflow

The workflow is illustrated in Figure 2. First, in the conceptual design phase, the primary specifications of the blade (such as radius, chord length, and so on) are considered, and values are determined to meet the feasible blade loading. Concurrently, design variables are defined to process optimization phase. As for optimization method, The Efficient Global Optimization (EGO) [5] is utilized by applying Kriging model. Initial sampling across the entire design space is performed using the Latin hypercube method, followed by an evaluation of propeller performance via CFD based on the goal function to capture overall trends. The next optimal point candidate is obtained based on the Distributed Genetic Algorithm (DGA), while adopting the Expected Improvement (EI) metric, and next round of CFD evaluation is conducted. This iterative process mechanically advances the propeller design.

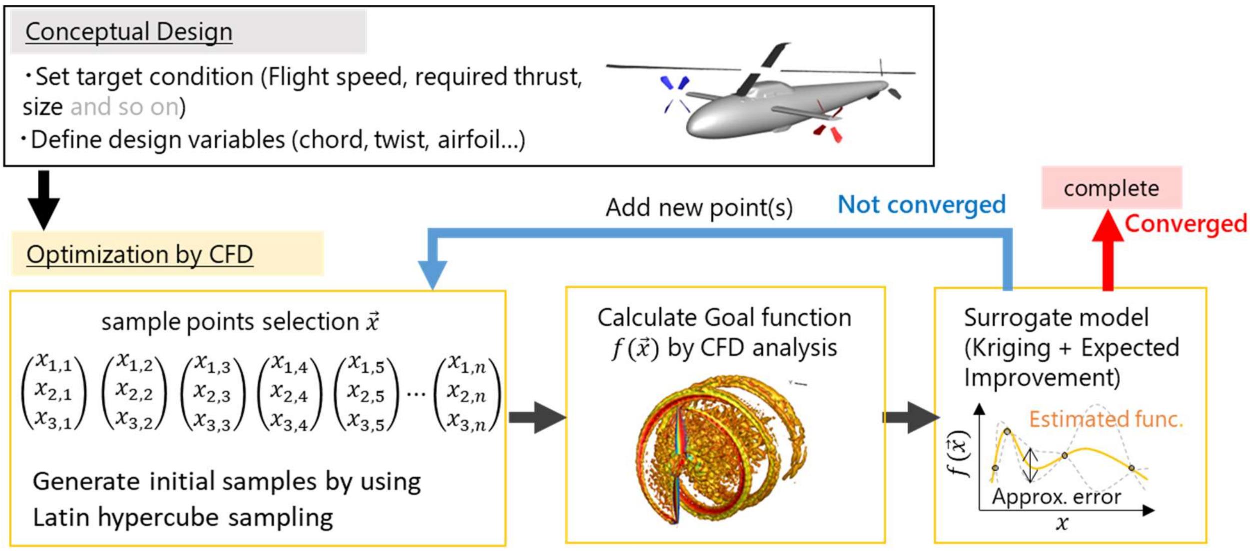

Figure 1 : Design workflow

3.2. CFD numerical setting

Simulation are performed using rFlow3D ([13], [14]), JAXA's in-house solver. This sovler is specialized for simulations of rotor blades and has the following features: direct representation of blade motion by the moving overlapped grid method, and low-dissipations over a wide Mach number range by evaluating the numerical flux using an all-speed scheme mSLAU and FCMT which is a spatial fourth-order accurate reconstruction method. It also has a trim analysis function that adjusts the thrust and moment of the aircraft to match the assumed flight conditions, making it a suitable solver for evaluating rotorcraft performance.

Table 1. specifications of rFlow3D

Governing equations	Three-dimensional compressible Navier-Stokes equations
Spatial discretization	Finite volume method
Time integration	4 stages Runge-Kutta (Background) Dual-time stepping, LU-SGS (Blade)
Viscous terms	2^{nd} order central difference method
Reconstruction	FCMT(4th-order compact MUSCL TVD)
Advection terms	mSLAU (modified SLAU)
Turb. model	①Design phase : SA Rotation correction (SA-R) ②Prediction for wind tunnel test Menter k-ωSST+γReθ transition model

3.3. Experimental setup

The wind tunnel test in this study has been conducted at JAXA's 2m × 2m Low-Speed Wind Tunnel [15]. This is a closed-circuit wind tunnel with a square cross-section measuring 2m × 2m. As shown in the test configuration in Figure 2, a rear-mounted robotic arm is placed within the wind tunnel, allowing the test model to be held in any desired orientation and position. The specifications of the wind tunnel facilities and test apparatus are summarized in Table 2. A nacelle-type propeller test apparatus was used as the mechanism for rotating the propeller, which was connected to the robotic sting via a six-component force balance. Both the propeller rotation speed and blade pitch angle can be set, and the pitch angle can be remotely adjusted during the test while measurements are being taken.

Table 2 : Wind tunnel test settings

Type	Closed circuit : Continuous, Atomospheric
Test section	2m x 2m square cross section, x 4m long
Wind speed	3 – 60m/s (continuous), max. 67m/s
Model support	Robotic model support system 6 degrees of freedom, capable of moving 1470 N, position precision ±0.5mm
Propeller drive unit	Motor : 7000W Propellr pitch angle : -30 - +60deg Rotation : max. 12000RPM

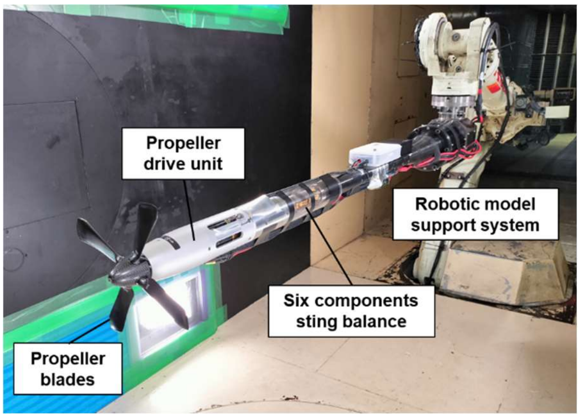

Figure 2 : Setup of a wind tunnel test for propeller performance measurement

4. DESIGN OF TAIL PROPELLER

The fundamental approach to propeller design follows the same principles as those used in the design of the side propellers in previous study [16]. In this paper, the design is extended to include the tail propeller. While the side propeller design considered the flight feasibility under both hover and cruise conditions, the tail propeller only operates during forward flight, then there is no need to consider hovering conditions for its design.

4.1. Conceptual design

The target flight speed of the assumed compound helicopter is 500 km/h, and the flyability at this speed should be considered. Figure 3 shows a top view of the rotorcraft. Ideally, the anti-torque of the main rotor is compensated by the vertical tail stabilizer, assuming equal thrust from the left and right side-propellers. (In practice, the thrust on the advancing side is greater than on the retreating side to generate the rotor's anti-torque.)

$$F_{fin} d = Q_{MR} \quad (1)$$

$$T_{adv} = T_{ret} \quad (2)$$

In determining the target thrust, it requires reference drag of overall rotorcraft system. As the flight speed increases, the parasite power becomes dominant [17], making it crucial to estimate the drag of the fuselage, rotor hub, wings and so on reasonably. Drag values of each component has been obtained from previous wind tunnel tests [18]. And the drag of the rotor is determined by referencing CFD results from previous investigation [19]. In the case of the winged compound helicopter studied here, there are three propellers, allowing some flexibility in the thrust share. This conceptual helicopter assumes electrically driven side propellers, which are expected to play a supplementary role compared to the tail propeller in terms of thrust generation in cruise flight. The thrust share has been set at 30% for the two side propellers and 70% for the tail propeller.

$$D_{total} = T_{adv} + T_{ret} + T_{tail} \quad (3)$$

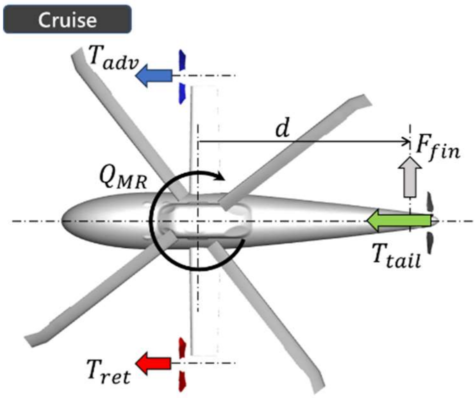

Figure 3 : Target flight condition (cruise)

Using target thrust value, the conceptual design of the tail propeller is proceeded. First, the radius can be largely determined by geometric constraints. It should be set to ensure that even with a 5-degree backward tilt when the rotorcraft is on the ground, the propeller tips do not touch the ground. Then, the tip speed must be determined to generate sufficient thrust during high-speed flight at 500 km/h, while also avoiding much noise. Since rotor noise levels are primarily dependent on tip speed [20], the tip speed of the tail propeller has been set to match that of the main rotor, with a tip Mach number (M_{tip}) of 0.65.

With this information, the target thrust coefficient can be fixed, and the solidity (= equivalent chord length) would be a variable to achieve an appropriate blade loading. For this design, the solidity is set to achieve $C_T/\sigma \fallingdotseq$ 0.1, where the airfoil performance is expected to be fully effective. As a result, the solidity, σ = 0.4, is larger compared to typical main rotors or tail rotors. To prevent an increase in pitching moment because of a small aspect ratio, a propeller with 6 to 8 blades seems appropriate, and in this case, an 8-blade configuration has been chosen. This design trend looks similar to the tail propeller of the SB>1 Defiant [3], which also aims for high-speed flight.

Table 3 : parameters/results of conceptual design

Aircraft weight	4000 kg
Flight condition	(1) Hover : V = 0 m/s (2) Cruise: V = 139 m/s (500 km/h)
Flight mission (Total time=1)	Hover time : t_h = 0.15 Cruise time : t_{FF} = 0.85
Main rotor	Radius : R_{MR} = 5.355 m Target Thrust (1) Hover : T_{MR}= 4000 kgf (2) Cruise : T_{MR}= 1200 kgf (30% of weight) Assumed Performance (1) Hover : FoM=0.64 (M_{tip} = 0.65) (2) Cruise : L/D_e= 3.5 (M_{tip} = 04875)
Propeller thrust share	T_{adv}: T_{ret} : T_{tail} = 0.15 : 0.15 : 0.7
Side prop	Radius : R_{SP} = 0.875 m Solidity : σ = 0.291 (4 blades) Airfoil : NACA0012 Tip speed : M_{tip}= 0.63 Target Thrust (1):hover : C_T/σ = 0.101 (2) cruise : C_T/σ = 0.038, J = 2.0
Tail prop (obtained in this study)	Radius : R_{TP} = 0.913 m Solidity : σ = 0.4 (8 blades) Tip speed : M_{tip}= 0.65 Airfoil : OAF117 Target Thrust : (2) Cruise : C_T/σ = 0.105, J = 2.0

4.2. Design variables for optimization

The design variables for the propeller are established based on previous study [16] on side propeller design. A summary of the design variables is shown in Figure 4 and Table 4. Three design variables are set for the twist and three for the chord (six in total). For the twist, a large linear twist over the blade span ranging from -30° to -50° is assumed to adjust high advance ratio conditions, with two control points positioned near the blade tip where the dynamic pressure get comparatively increased. Regarding the chord, the position of chord1 can be set at dv6, allowing both tapered and reverse-tapered shapes to emerge as potential design solutions.

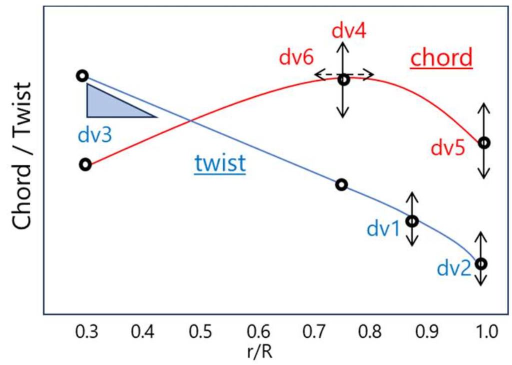

Figure 4 : Design variables overview

Table 4 : setting of design variables

	Design variables	Range
dv1	Twist1@ r/R = 0.875	-5°~ 5°
dv2	Twist2@ r/R = 1.0	-10°~ 0°
dv3	Linear Twist	-50°~ -30°
dv4	Chord1 @dv6	$1.0c_{ref}$ ~ $1.5c_{ref}$
dv5	Chord2 @ r/R = 1.0	$0.5c_{ref}$ ~ $1.0c_{ref}$
dv6	Position of Chord1	0.4 ~ 0.85 r/R

4.3. Design results

For the design space previously presented, 40 initial samples are obtained using the Latin hypercube method, and CFD analysis has been performed under the design thrust condition (C_T/σ = 0.105) based on the cruise condition (see Figure 5). The additional samples generated through optimization are indicated by the legend "add samples," from which the design solution with the highest propeller efficiency was selected as the optimal blade (OPT-TP). Compared to the baseline tail propeller (BLN-TP), a performance improvement of approximately 3% is achieved. To compare the shapes, the twist angle distribution is shown in Figure 6, where a significant twist reduction has been applied to better suit high advance ratio conditions, with additional twist introduced near the blade tip. In subsequent chapters, the performance of this design would be further validated through wind tunnel testing.

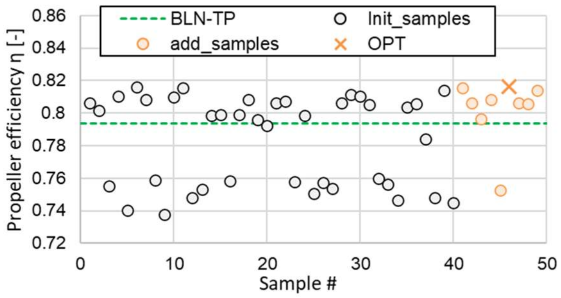

Figure 5 : Optimization blade samples

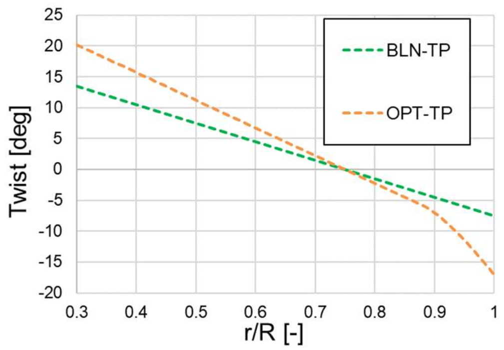

Figure 6 : Twist distributions for tail propellers

5. RESULTS AND DISCUSSIONS

5.1. Propeller performance

The optimal tail propeller's shape obtained in chapter 4 and the side props for adv/ret-side from previous study are subjected to wind tunnel tests to measure performance. The planforms of propeller blades, including the baseline shapes, are shown in Figure 7. Due to the limitations of the scale of wind tunnel facilities, these propellers have been manufactured at a 1/7 scale from the original designs. The three types of side propellers (BLN-SP, Adv-OPT, Ret-OPT) have a radius of R = 0.125 m, while the two types of tail propellers (BLN-TP, OPT-TP) have a radius of R = 0.131 m. It should be noted that the propeller wind tunnel test apparatus used (see Figure 2) is designed for four-blade propellers, whereas the optimal tail propeller OPT-TP was designed as an eight-blade propeller. Therefore, the tests were conducted using a four-blade configuration. To take into account for the difference in the number of blades, the propeller efficiency would be evaluated by determining the target thrust using blade loading, a parameter obtained by dividing the thrust coefficient by solidity.

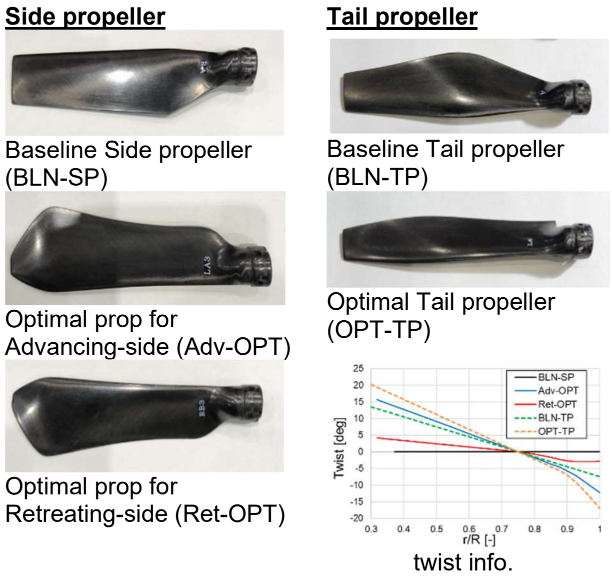

Figure 7 : Pictures of Propeller models for wind tunnel test

The summary of the wind tunnel test case conditions conducted in this study is presented in Table 5. In each case, the wind speed and rotational speed are fixed, and the thrust is adjusted by varying the propeller pitch angle during cases, thereby obtaining the performance curves.

The test conditions have been designed to ensure that the Reynolds number based on the equivalent chord being compared remained nearly identical, and the wind tunnel wind speed and rotational speed have been accordingly set. The Reynolds number ranges from Re = 5.0e4 to 1.3e5. It should be noted that, compared to the full-scale, the dimensions are at 1/7 scale, and the tip speed is less than one-third, resulting in Reynolds numbers that differ by an order of magnitude from those in the design phase.

Figure 8 and Figure 9 respectively show the performance curves for the side propellers and the tail propellers. Under hovering conditions, the Figure of Merit would be applied, while for forward flight conditions with an advance ratio J = 0.4 to 2.0, propeller efficiency would be used. The horizontal axis is standardized using blade loading. For reference, CFD analyses are conducted under these wind tunnel test conditions, and the CFD results are presented alongside the wind tunnel test results.

5.1.1. Side propellers

The baseline side propeller has a tapered chord and twist-free design, which ensures that both normal and reverse pitch angles can be used during hovering without significant performance differences between the left and right propellers. In contrast, the Adv-OPT and Ret-OPT propellers have a reverse-tapered planform, with the twist distribution differing between the two propellers On the advancing side of the rotorcraft, where thrust is generated towards the front, the Adv-OPT design includes a significant twist down over the span. Conversely, on the retreating side, where reverse pitch is required during hovering, the Ret-OPT has a more modest tip-down twist.

The impact of these designs is particularly evident in the hovering case. While the Adv-OPT shows improvement in the Figure of Merit (FoM), the Ret-OPT, tested with reverse pitch (as noted in Table 5), exhibits a worsening FoM compared to the BLN-SP due to the tip-down twist. This trend is confirmed by both CFD and wind tunnel tests. On the other hand, during forward flight, where thrust is directed towards the front of the rotorcraft, it improves forward flight performance, leading to a significant increase in propeller efficiency for both Adv-OPT and Ret-OPT compared to the baseline blade.

Overall, the performance of the Adv-OPT blade surpasses the other two designs. However, at a lower advance ratio (J = 0.4), under conditions of low thrust, () the Ret-OPT shows the highest performance, a trend observed in both wind tunnel tests and CFD analysis. Although there are quantitative differences, the overall trends show good agreement.

5.1.2. Tail propeller

The tail propeller designed in Chapter 4 was also evaluated for its performance. To withstand the high blade loading under high advance ratio conditions, a greater twist was applied compared to the baseline propeller (BLN-TP). Similar to the side propellers, while the BLN-TP performed better under low advance ratio conditions, the increase in propeller efficiency for the OPT-TP became more pronounced as the advance ratio increased. This trend was observed in both CFD and wind tunnel tests. However, the CFD results showed no significant performance degradation under high blade loading conditions, or the degradation appeared much later than in the wind tunnel tests. Despite using a transition model in the analysis to account for low Reynolds number flows, the use of RANS equations likely limits the accuracy of the predictions.

Table 5 : Wind tunnel Test (&CFD simulation) matrix

Blade	Rotation [RPM]	Inflow [m/s]	Reynolds # (chord base)	Advance ratio J
Baseline side propeller (BLN-SP)	5500 (Mtip = 0.212)	0	1.2e5	0 (hover)
$R_{SP} = 0.125\ m$	5500 (Mtip = 0.212)	9.2	1.2e5	0.4
$c_{eq} = 0.0257\ m$	5500 (Mtip = 0.212)	18.3	1.3e5	0.8
	4000 (Mtip = 0.154)	20	9.5e4	1.2
	3000 (Mtip = 0.115)	20	7.5e4	1.6
	2400 (Mtip = 0.092)	20	6.3e4	2.0
Optimal prop for Advancing-side (Adv-OPT)	5000 (Mtip = 0.192)	0	1.2e5	0 (hover)
$R_{SP} = 0.125\ m$	5000 (Mtip = 0.192)	8.4	1.2e5	0.4
$c_{eq} = 0.0286\ m$	5000 (Mtip = 0.192)	16.7	1.3e5	0.8
	3600 (Mtip = 0.138)	18.2	9.6e4	1.2
	2750 (Mtip = 0.106)	18.2	7.6e4	1.6
	2200 (Mtip = 0.085)	18.2	6.5e4	2.0
Optimal prop for Retreating-side (Ret-OPT)	5000 (Mtip = 0.192)	0	1.2e5	0 (hover*)
$R_{SP} = 0.125\ m$	5000 (Mtip = 0.192)	8.4	1.2e5	0.4
$c_{eq} = 0.0286\ m$	5000 (Mtip = 0.192)	16.7	1.3e5	0.8
	3600 (Mtip = 0.138)	18.2	9.6e4	1.2
	2750 (Mtip = 0.106)	18.2	7.6e4	1.6
	2200 (Mtip = 0.085)	18.2	6.5e4	2.0
Baseline tail propeller (BLN-TP)	4500 (Mtip = 0.181)	7.9	1.0e5	0.4
$R_{TP} = 0.131\ m$	4500 (Mtip = 0.181)	15.7	1.1e5	0.8
$c_{eq} = 0.0252\ m$	3100 (Mtip = 0.125)	16.4	7.6e4	1.2
	2350 (Mtip = 0.095)	16.4	6.0e4	1.6
	2100 (Mtip = 0.085)	16.4	5.5e4	1.8
	1900 (Mtip = 0.077)	16.4	5.1e4	2.0
Optimal tail propeller (OPT-TP)	5500 (Mtip = 0.222)	0	1.0e5	0.4
$R_{TP} = 0.131\ m$	5500 (Mtip = 0.222)	9.6	1.0e5	0.8
$c_{eq} = 0.0208\ m$	3800 (Mtip = 0.153))	19.2	1.1e5	1.2
	2850 (Mtip = 0.115)	20	7.7e4	1.6
	2550 (Mtip = 0.103)	20	6.0e4	1.8
	2300 (Mtip = 0.093)	20	5.1e4	2.0

*use reverse pitch angle for negative thrust generation

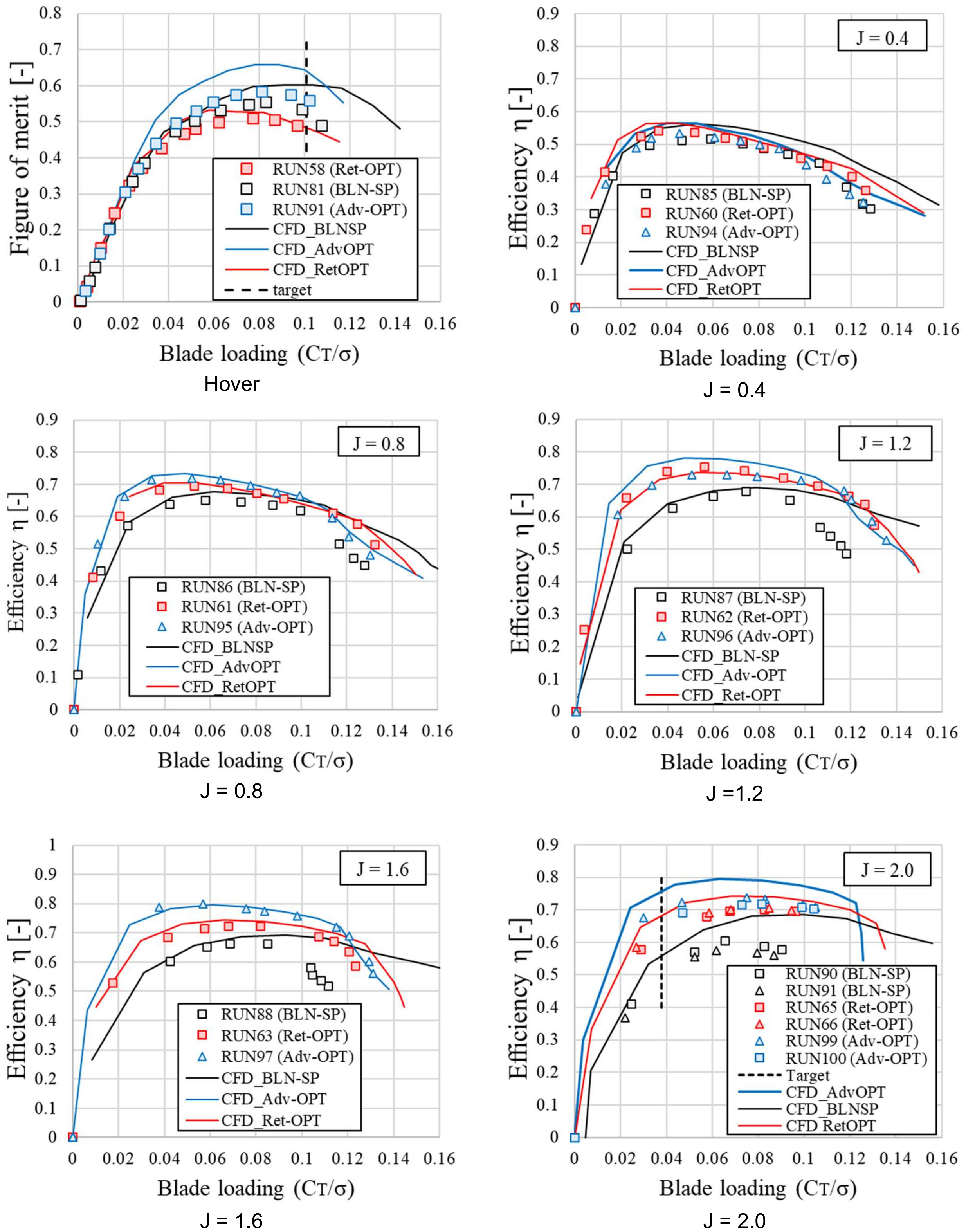

Figure 8 : Blade loading vs Propeller efficiency (Side propellers, EXP&CFD results)

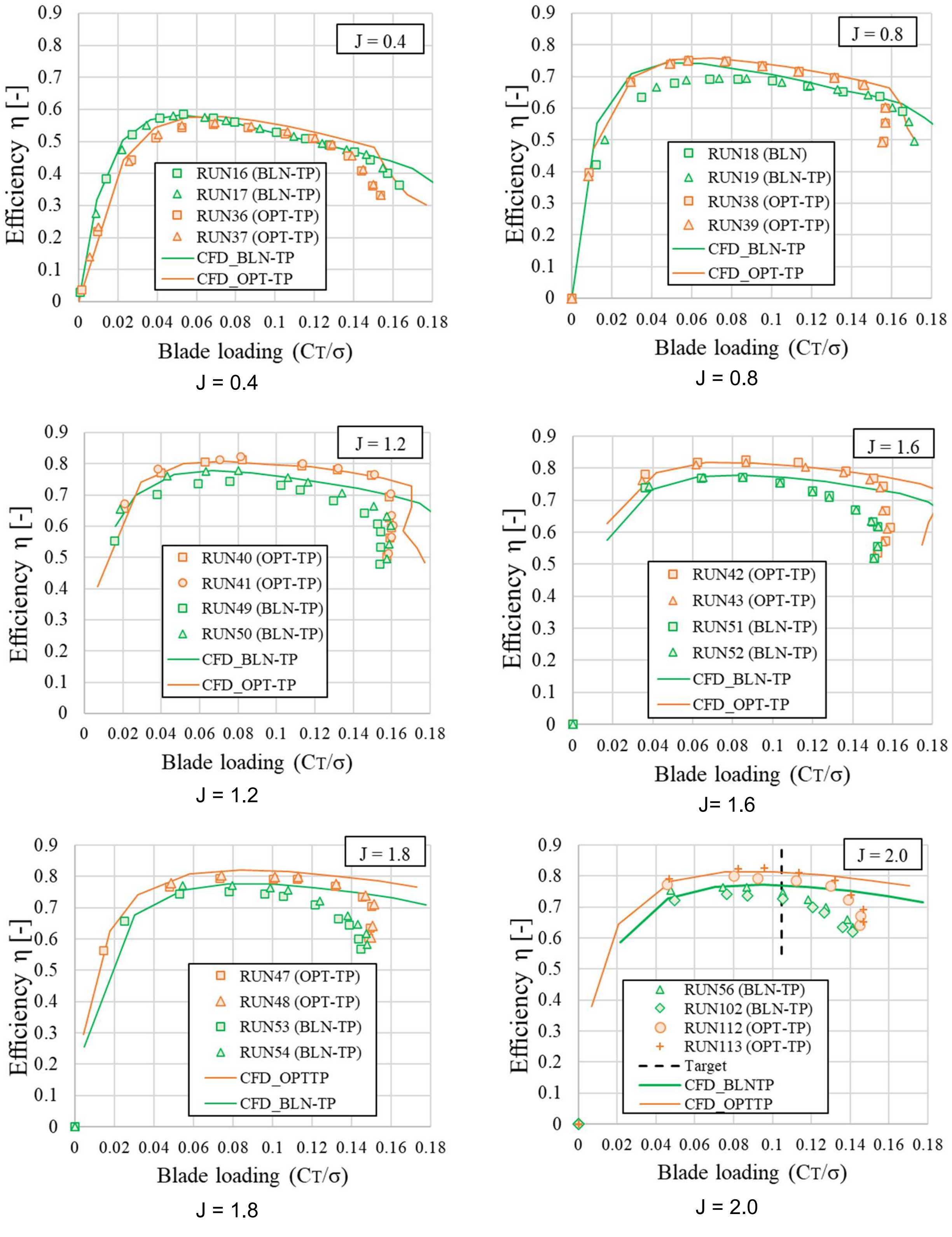

Figure 9: Blade loading vs Propeller efficiency (Tail propellers, EXP&CFD results)

5.2. Overall system performance

Using the evaluated propeller performance values, the potential fuel savings effect when applied to the assumed winged compound helicopter can be examined. Based on the performance curves shown in Figure 8 and Figure 9, the figure of merit and propeller efficiency at the design target blade loading values (refer to Table 3) are summarized in Table 6.

There are two sets of results, those from the wind tunnel tests and the CFD analysis used to evaluate the impact on the overall aircraft system performance. Overall, the CFD results tend to be overestimated compared to the test. However, considering that the Reynolds numbers in the wind tunnel tests are on the order of 10e4 to 10e5, the wind tunnel results reflect conditions under which the airfoil performance may degrade [21], making accurate performance evaluation via RANS analysis challenging in this regime. Nonetheless, there is no reversal in the ranking order among the propellers being compared, suggesting that qualitatively comparable results can be expected.

Table 6 : Summary of propeller performance under design conditions

	Figure of Merit	Propeller efficiency @Cruise J =2.0
BLN-SP	0.603 (CFD)	0.559 (CFD)
	0.524 (EXP)	0.476 (EXP)
Adv-OPT	0.640 (CFD)	0.757 (CFD)
	0.562 (EXP)	0.689 (EXP)
Ret-OPT	0.483 (CFD)	0.710 (CFD)
	0.484 (EXP)	0.616 (EXP)
BLN-TP	-	0.770 (CFD)
		0.737 (EXP)
OPT-TP	-	0.812 (CFD)
		0.803 (EXP)

To compare the reduction effects of the optimally designed propellers, two configurations of rotorcrafts, as shown in Figure 10, would be considered. The total power consumption during hovering and forward flight have been calculated and compared. The flight conditions, as outlined in Table 3, were based on calculations for a 4-ton-class compound helicopter. It is important to note that the main rotor performance is assumed to be constant, as the design specifications.

Power consumption during hovering is shown in Figure 11 (1). While hovering, the side propellers are used to generate anti-torque for the main rotor. The tail propeller is not used in this phase and is therefore excluded from the analysis. Although the power consumption of the Ret-OPT propeller increases, causing a slight increase in the total power consumption of the side propellers, the main rotor's power consumption dominates the overall power consumption, making the impact relatively minor.

Next, the power consumption during forward flight at a speed of 500 km/h would be evaluated, with the results presented in Figure 11 (2). Based on the thrust share shown in Table 3, the three propellers compensate the total drag of the rotorcraft, and the main rotor's shaft power is added to estimate the overall power consumption. Focusing on the breakdown in the graph, the tail propeller, which has a larger share of the thrust distribution, accounts for about 60% of the total power consumption. This indicates that in forward flight, the performance improvement of the tail propeller significantly benefits the system performance, making it a critical design factor. Although there is a slight deterioration in hovering performance when comparing the BLN-config and OPT-config, in forward flight case, a total fuel efficiency improvement of approximately 15% can be expected in the wind tunnel test results (EXP), and approximately 11% based on the CFD results.

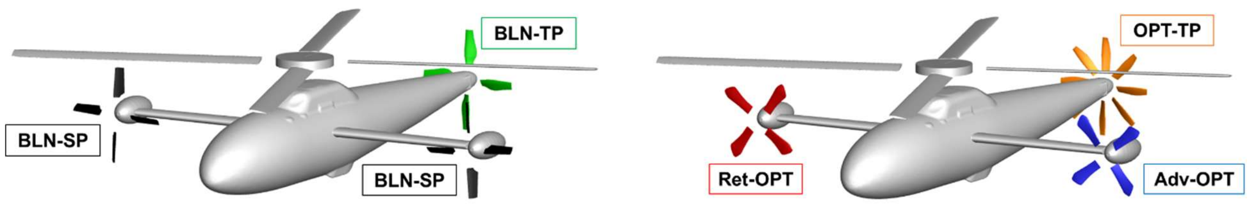

Baseline configuration (BLN-config)　Optimal configuration (OPT-config)

Figure 10 : Comparison of BLN/OPT configurations

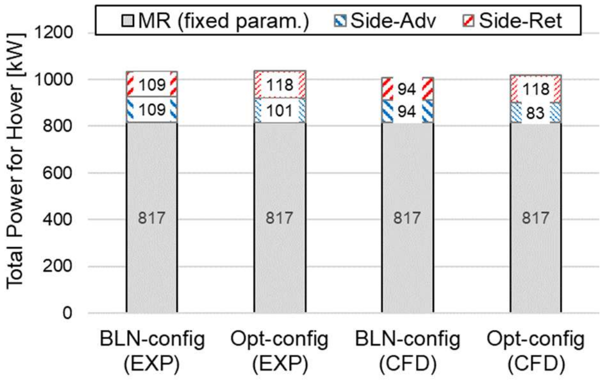

(1) Total consumption power in Hover
(For main rotor (MR) uses fixed value)

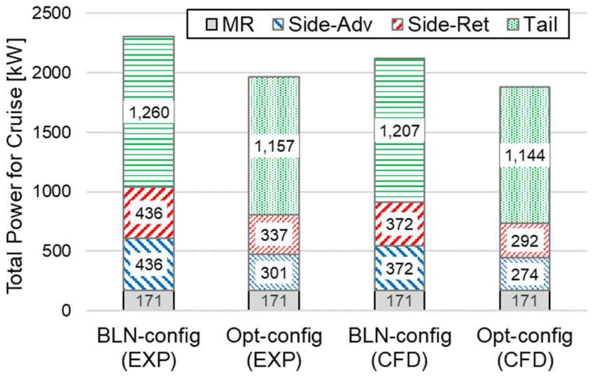

(2) Total consumption power in Cruise
(For main rotor (MR) uses fixed value)

Figure 11 : Estimated power consumptions under hovering and cruise conditions (BLN-config vs OPT-config / EXP vs CFD)

6. CONCLUDING REMARKS

In this study, an optimal propeller design and performance evaluations for the JAXA concept winged compound helicopter were conducted using both wind tunnel testing and CFD analysis. The conclusions and summary are as follows:

1. A procedure for designing the tail propeller to compensate for the total drag of the rotorcraft under the target flight condition (forward flight at 500 km/h) has been presented. As a result, an 8-blade tail propeller with a solidity of σ = 0.4 is obtained. This high solidity blade aligns with current trend in tail propeller for an existing high-speed helicopter.
2. Through optimal design using EGO and CFD, a design solution of a tail propeller has been obtained with approximately 3% improvement in propeller efficiency. These values under the design thrust condition has been evaluated using both wind tunnel testing and CFD, confirming the performance improvement over the baseline propeller.
3. The performance of the side propellers designed in previous study are also validated through wind tunnel testing. As anticipated in the design phase, the performance trends are in line with the concept: a propeller for the advancing side that promises significant performance improvements in both hovering and cruise conditions, and a propeller for the retreating side that improves efficiency in cruise while slightly compromising the Figure of Merit (FoM) during hovering.
4. The fuel-saving effects of optimally designed side and tail propellers have been investigated, focusing on the overall system power consumption of the rotorcraft, including the main rotor. Both of experimental/numerical results demonstrate that the three propellers designed through this series of studies can reduce overall power consumption during forward flight by approximately 10% from the baseline configuration.

Future work will need to explore additional wind tunnel testing under conditions with higher Reynolds numbers and/or CFD analysis without relying on turbulence models to improve the agreement with low-Reynolds number conditions. This should help in achieving a deeper understanding of the propeller performances in a full-scale helicopter.

7. REFERENCES

[1] Y. Tanabe, T. Aoyama, N. Kobiki, M. Sugiura, R. Miyashita, S. Sunada, K. Kawachi , M. Nagao, “A Conceptual Study of High Speed Rotorcraft,” 40th European Rotorcraft Forum, Southampton, UK, September, 2014.

[2] "Airbus Racer speeds past 400 km/h," AIRBUS, 23rd July 2024. [Online]. Available: https://www.airbus.com/en/newsroom/press-releases/2024-07-airbus-racer-speeds-past-400-kmh. [Accessed 18th Aug. 2024].

[3] LOCKHEED MARTIN, "SB>1 DEFIANT® The Next Generation is Here," [Online]. Available: https://www.lockheedmartin.com/en-us/products/sb1-defiant-technology-demonstrator.html. [Accessed 18th 8 2024].

[4] KHI, "Kawasaki Succeeds in Flight Test of the Unmanned Compound Helicopter K-RACER," [Online]. Available: https://www.khi.co.jp/pressrelease/detail/20201006_1.html. [Accessed 14 9 2023].

[5] M. Kanzaki, S. Jeong , M. Murayama, “High-Lift System Optimization Based on Kriging Model Using High Fidelity Flow Solver,” Transaction of the Japan Society for Aeronautical and Space Science, Vol. 49, No. 165, 2006.

[6] G. Wilke, J. Bailly, K. Kimura , Y. Tanabe, “JAXA-ONERA-DLR cooperation: results from rotor optimization in hover,” CEAS Aeronautical Journal, 13(2):1-21, 2022.

[7] K. Kimura, G. Wilke, J. Bailly , Y. Tanabe, “JAXA-ONERA-DLR COOPERATION: RESULTS FROM ROTOR OPTIMIZATION IN FORWARD FLIGHT,” 48th European Rotorcraft Forum, Winterthur, Switzerland, 2022.

[8] J. Bailly, G. Wilke, K. Kimura , Y. Tanabe, “JAXA-ONERA-DLR COOPERATION: RESULTS FROM MULTI-POINT AERODYNAMIC OPTIMIZATION OF A ROTOR IN HOVER AND FORWARD FLIGHT,” 49th European Rotorcraft Forum, Bückeburg, Germany, 2023.

[9] M. Byung-Young, A. F. Dunn, A. Gao, V. Klimchenko, C. G. Matalanis , B. E. Wake, “High Speed and Highly Efficient Rotor Blade Design,” 78th Vertical Flight Society Annual Forum, Texas, FortWorth, 2022.

[10] B. G. v. d. Wall, C. Kessler, Y. Delrieux, P. Beaumier, M. Gervais, J.-F. Hirsch, K. Pengel , P. Crozier, “From ERATO basic research to the blue EdgeTM rotor blade,” American Helicopter Society 72nd Annual Forum, West Palm Beach, Florida. 2016., 2016.

[11] M. Sugiura, Y. Tanabe, H. Sugawara , K. Takekawa, “Optimal Design of Rotor Blade for a Winged Compound Helicopter at High Advanced Ratio,” Vertical Flight Society 76th Forum, Oct. virtual, 2020.

[12] K. Kimura, M. Sugiura, H. Sugawara , Y. Tanabe, “Flight Testing of Optimal Blade for a High-Speed Helicopter,” 79th Vertical Flight Society Annual Forum & Technology Display, West Palm Beach, United States, 2023.

[13] Y. Tanabe , S. Saito, “Significance of All-Speed Scheme in Application to Rotorcraft CFD Simulations,” 3rd International Basic Research Conference on Rotorcraft Technology, Nanjing, China, October 14-16, 2009., 2009.

[14] Y. Tanabe, S. Saito , H. Sugawara, “Evaluation of Rotor Noise Reduction by Active Devices Using a CFD/CSD Coupling Analysis Tool Chain,,” Proceedings of 1st Asian/Australian Rotorcraft Forum, ARF 2012 Executive Committee Paper A-IV-1_P107_F, Busan, K,, 2012.

[15] "Test facilities - 2mx2m Low-speed Wind Tunnel," 18th Aug. 2024. [Online]. Available: https://www.aero.jaxa.jp/eng/facilities/windtunnel/. [Accessed 14 9 2023].

[16] K. Kimura, Y. Tanabe , H. Sugawara, “Optimal Design of Side Propellers for a Winged Compound Helicopter,” 9th Asian/Australian Rotorcraft Forum, Novermber, Nanjing, China, 2023.

[17] J. G. Leishman, Principles of Helicopter Aerodynamics : second edition, CAMBRIDGE uniersity press, ISBN 0-521-85860-7, 2006.

[18] N. Kobiki, Y. Tanabe, H. Sugawara, K. Kimura , M. Sugiura, “An Aerodynamic Study for the 3rd Configuration of JAXA High Speed Compound HelicopterJAXA,” JOURNAL OF THE JAPAN SOCIETY FOR AERONAUTICAL AND SPACE SCIENCES, 2021.

[19] K. Kimura, Y. Tanabe , M. Sugiura, “The Effect of Blade Tip Sweep Angle on Forward Flight Performance of a High-speed

Helicopter," 78th VFS Forum, Fortworth, 2022.

[20] F. Farassat, R. J. Pegg and D. A. Hilton, "Thickness Noise of Helicopter Rotors at High Tip Speeds," AIAA 2nd Aero-Acoustics Conference March 24-26, 1975 Hampton, Virginia, 1975.

[21] "Airfoil tools," 18th Aug. 2024. [Online]. Available: http://www.airfoiltools.com/index.